CrossMark

ORIGINAL ARTICLE

Porphyrin acidity and metal ion coordination revisited: electronic substitution effects

Svetlana G. Pukhovskaya[1] · **Dao Tkhe Nam**[1] · **Yulia B. Ivanova**[2] ·
Lizaveta S. Liulkovich[3] · **Alexander S. Semeikin**[1] · **Sergei A. Syrbu**[1] ·
Mikalai M. Kruk[3]

Abstract Macrocycle acidity and Zn^{2+} ion coordination are reported for three porphyrin derivatives which differ in both steric and electronic substitution effects on the macrocycle π-conjugated system. The role of the electronic substitution effects in the macrocycle deprotonation and metal ion chelating was found to be dominating whereas the macrocycle nonplanar distortions contribute to the acidity and metal chelation rate of the studied porphyrins in less extent. The contributions of both resonance and inductive electronic substitution effects have been distinguished based on the relationship between the weighted sum of resonance and inductive Hammett constants and the acidity and metal ion chelation rate.

Keywords Porphyrins · Acid-base equilibria · Substitution effect · Molecular orbitals · Conformation · Metal complexation

✉ Sergei A. Syrbu
syrbu@isuct.ru

✉ Mikalai M. Kruk
krukmikalai@yahoo.com; m.kruk@belstu.by

1 Ivanovo State University of Chemistry and Technology, Sheremetevsky Str. 7, Ivanovo, Russian Federation 153000

2 G.A. Krestov Institute of Solution Chemistry of Russian Academy of Sciences, Academicheskaya Str. 1, Ivanovo, Russian Federation 153045

3 Belarusian State Technological University, Sverdlova Str. 13a, 220006 Minsk, Belarus

Introduction

Development of new macroheterocyclic compounds with definite optical properties and/or chemical reactivity to be used in the design of new advanced materials is a interdisciplinary problem of high priority. Molecular structure of tetrapyrrolic macrocycles allows suggesting the diversity of new compounds by means of fine tuning of their properties with modification of the peripheral substitution pattern, formation of chelated complexes with metal ions and axial ligation of the latter [1, 2]. In most of cases electronic effects arising upon peripheral substitution on the π-conjugated system of macrocycle interfere with concomitant sterical effects. Therefore the discrimination between these two contributions needs the detailed consideration in the each particular case to establish properly the structure–property relationship.

Tetrapyrrolic macrocycles are known to be amphoteric compounds, possessing both basic properties, involving the protonation of the pyrrolenic (–N═) nitrogens and acidic ones, involving the proton removing from pyrrolic (–NH–) nitrogen atoms [2–5]. Depending the acidity (basicity) of the microenvironment both mono- and doubly (de)protonated species are formed, which are in equilibrium. The ionic (i.e. protonated and deprotonated) species are chemically stable, and their stabilization is due to the electronic, solvation and steric factors [5]. Electronic factors of stabilization arise from the redistribution of the electron density over π-conjugated system of macrocycle, as well as between the macrocycle and peripherical substituents, upon attachment/release of the protons to/from the macrocycle core. Solvation effects on stabilization are due to the rearrangement of the solvation shell which includes the specific interactions of the polar molecular fragments with the solvent molecules. These weak

interactions include also the associative interactions with acid counter ions, which are of particular importance in the case of low polar and poorly solvating solvents [5, 6]. The steric factors of stabilization are, in fact, the structural relaxations of macrocycle itself or between the macrocycle and the substituents attached via spacers, allowing to latters some degree of freedom. These structural rearrangements are coupled with solvent shell reorganization and are aimed to adopt the minimum potential energy of the molecule.

Recently, we have started the studies in the direction of exploitation of unique physico-chemical properties of deprotonated tetrapyrrolic macrocycles for the development of the new efficient approach to the synthesis of metallocomplexes and design of new sensing devices for the detection of the substrates bearing positive charge [7–9]. The 1,8-diazabicyclo-[5,4,0]-undec-7-en (DBU) has been applied as deprotonating agent. The formation of metallocomplexes when metal salts react with doubly deprotonated macrocycle after the addition of DBU has been documented and the advantages of such an approach have been discussed [7–9]. In these studies the main attention was paid to the identification and assignment of the species formed under the reactions of deprotonation and metal chelating, and comparison of the reaction rate for the metallocomplexes formation in cases of molecular mechanism of the reaction (i.e., when metal salts react with the porphyrin free base) and the ionic one, where a ion interacts with deprotonated macrocycle. The problem of the structure–property relationship received much less attention there [7–9]. The case under consideration is quite complicated, since all the three listed above factors stabilizing the deprotonated forms are able to contribute to the reactions rate. The solvation effects may be quite easily isolated by conducting the reaction in different solvents, followed with correlation of the reaction rates with physico-chemical properties of solvents. To separate the electronic and steric contributions to the rate of the deprotonation and metal ion chelating, a special series of compounds need to be used.

Thus, in the given study we make the comparison between three porphyrins which differ in both the electronic communication between the macrocycle and substituents and the steric interactions. The substitution with groups possessing both the inductive and mesomeric (resonance) effects of different sign has been applied. Relative importance of the electronic communication of peripheral substituents via the π-conjugated system of macrocycle or the macrocycle σ-bonds polarization will be analyzed. Moreover, substitution at the 2,3,7,8,12,13,17,18 *β*-positions of pyrroles and 5,10,15,20-*meso*-positions may bring nonequivalent contributions due to the different electronic density of corresponding molecular orbitals on the macrocycle atoms. Beside this,

the dodecasubstitution pattern enables us to modulate the steric interactions due to the close proximity of the neighboring substituents with moderate bulkiness.

Experimental

Equipment

NMR spectra were acquired on the commercial instrument Bruker Avance 500 MHz and chemical shifts (δ) are reported in parts per million (ppm) referenced to tetramethylsilane (TMS) or the internal (NMR) solvent signals. Mass spectra were run using a HP5989A apparatus (CI and EI, 70 eV ionisation energy) with Apollo 300 data system or a Thermo Finnigan LCQ Advantage apparatus. Ground state absorption spectra, spectrophotometric titration experiments and kinetic measurements were carried out with spectrophotometer Shimadzu UV-1800. The methods of the titration procedure and protocols of experimental data analysis were described in our previous papers [7–10]. The relative uncertainty in determined acidity constants did not exceeded 5%.

Reagents

$Zn(OAc)_2$ "for analysis" was purified by recrystallization from acetic acid followed by dehydration at 380–390 K according to methods described [11]. Dry acetonitrile (water content no more than 0.03%) was used in the titration experiment. The deprotonating agent 1,8-diazabicyclo-[5,4,0]-undec-7-en (DBU) was used as received ($pK_a = 13.2$ in acetonitrile) [12]. The concentration of working solutions of DBU in CH_3CN was 0.01 M in all the cases. The titrant concentration was chosen so that the total change in the solution volume by the end of titration did not exceed 1%.

Synthesis

2,3,7,8,12,13,17,18-octabromo-5,10,15,20-tetrakis(trifluoromethyl)porphine (**I**) was prepared according to procedure described in Ref. [10]. The compound was isolated by column chromatography (silica gel, eluted with cyclohexane) followed with recrystallization (from CH_2Cl_2 with slow diffusion of MeOH). Elem.anal.: calcd. for $C_{24}H_2N_4Br_8F_{12}$: C, 23.75; H, 0.16; N, 4.61; found: C, 23.69; H, 0.17; N, 4.63. ^1H NMR (500 MHz, $CDCl_3$, TMS) δ(ppm): −1.63 (s, 2H, NH); Abs.: ($CHCl_3$), λ_{max}, nm (log ε): 433 (4.87); 636 (4.09). MALDI-TOF-MS (m/z): found 1213.18 [M+H]+, calcd. 1213.56.

2,3,7,8,12,13,17,18-octabromo-5,10,15,20-tetrakis(phenyl)porphine (**II**) was prepared by a bromination reaction of 5,10,15,20-tetrakis-tetraphenylporphyrinato copper(II) complex followed by an acid demetalation

reaction according to Ref. [11]. Compound was isolated by column chromatography (Al$_2$O$_3$, type III by Brockman, eluent chloroform:benzene 1:1). ^{1}H NMR (500 MHz, CDCl$_3$, TMS) δ(ppm): 8.21 (m, 8H, phenyl o-H), 7.79 (m, 12H, phenyl m- and p-H), -1.65 (bs, 2H, NH). Elem.anal.: calcd for C$_{44}$H$_{22}$N$_4$Br$_8$: C, 42.42; H, 1.78; N, 4.49; Br, 51.30; found: C, 42.35; H, 1.90; N, 4.40; Br, 51.32. Abs.: (toluene) λ$_{max}$, nm (log ε): 470 (5.25); 622 (4.10); 738 (3.85). MALDI-TOF-MS (m/z): found 1245.51 [M+H]+, calcd. 1245.96.

5,10,15,20-tetrakis(trifluoromethyl)porphine (**III**) was prepared as described in Ref. [9] and was purified by column chromatography (silica gel, eluent hexane–benzene 10:1) followed with recrystallization from the methylene chloride–methanol mixture. Elem.anal.: calcd. for C$_{24}$H$_{10}$N$_4$F$_{12}$: C, 49.50; H, 1.73; N, 9.62; found: C, 49.53; H, 1.64; N, 9.33. ^{1}H NMR δ(ppm): 9.60 (s, 8H), −2.08 (s, 2H, NH); Abs.: (CH$_2$Cl$_2$), λ$_{max}$, nm (log ε): 403 (5.08), 510 (3.97), 545 (3.97), 593 (3.67), 649 (4.00). MALDI-TOF-MS (m/z): found 582.01 [M+H]+, calcd. 582.35.

Molecular structures of studied porphyrins are shown on the Scheme 1.

Results and discussion

Conformation, electronic structure and absorption spectra

All the studied porphyrins can be divided into two groups according to the molecular structure: the first one consist of porphyrins **I** and **II**. These compounds are heavily substituted at 12 peripheral positions and, as many other known dodecasubstituted porphyrins, [13 and Refs. 2b, 5–13 therein, 14] must have the *saddle*-type distorted macrocycle with moderate magnitude of distortion. On the contrary, the porphyrin **III** has four *meso*-trifluoromethyl groups, and the sterical interactions of fluorine atoms with adjacent pyrrole protons are rather weak to induce pronounced nonplanar distortions. This porphyrin has barely visible macrocycle ruffling and is considered to be nearly planar. The electronic structures of all these compounds bear similar features. According to Gouterman four-orbital model mutual positioning of two highest occupied molecular orbitals (HOMO) depends on the substitution pattern: introducing the electron donating/withdrawing substituents at any position leads to the increase/decrease in the energy of molecular orbital having non-zero electron density at these atom positions. Substitution at the *meso*-positions mainly affects the energy of b$_{1u}$ orbital (D$_{2h}$ point symmetry group notation) since it has the maxima of electronic density at *meso*-carbons. The energy of this orbital is also affected with metal ion chelating since this orbital has also the maxima of electronic density at the pyrrolic nitrogens. The energy of a$_u$ orbital is not affected upon *meso*-substitution, since this orbital has nodes at *meso*-carbons. On the contrary, the a$_u$ orbital has maxima at pyrrolic rings; therefore its energy can be selectively tuned by pyrrole substitution. The architecture of substitution, we have used for the studied compounds, led to the changes in energy gap between HOMO orbitals, but their order remained unchanged in all three cases, i.e. E(a$_u$) > E(b$_{1u}$).

Ground state absorption spectra (Table 1) reflect both the pure electronic effects and the effects originating from the nonplanar macrocycle distortions. Now it is accepted, that nonplanar distortions themselves do not induce directly the changes in the electronic spectra, but their influence is mediated by the induced perturbations in the π-conjugated system of macrocycle [15, 16]. In other words, the spectral changes do not depend on the magnitude of the distortions as they are, but on the influence of the distortions on the electronic structure of molecule. Therefore, the spectral shifts values do not exactly correlate with the trends derived for the HOMO orbitals.

I   **R** = -CF$_3$

     R$_1$ = -Br

II   **R** = -C$_6$H$_5$

     R$_1$ = -Br

III   **R** = -CF$_3$

     R$_1$ = -H
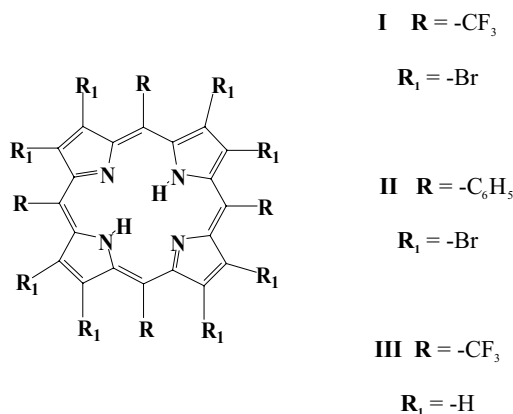
Scheme 1 Molecular structures of studied porphyrins

Table 1 Spectral features and overall acidity constants p$K_{a1,2}$ of all the studied porphyrins

Compound	λ$_{max}$, nm (lgε)	p$K_{a1,2}$
H$_2$PI	435 (5.0), 639 (4.1)	6.78
H$_2$PII	470 (5.25), 568 (3.95) 622 (4.10), 738 (3.85)	10.77
H$_2$PIII	400 (5.23), 509 (4.14) 544 (4.13), 591 (3.84), 647 (4.11)	9.69
PI$^{2−}$	483 (4.6)	
PII$^{2−}$	497 (5.30), 774 (4.80)	
PIII$^{2−}$	431 (4.96), 598 (4.00), 717 (3.89)	

Spectra for the free bases and the doubly deprotonated species are measured in acetonitrile and in the acetonitrile-DBU system, respectively

Acidity and formation of deprotonated species

Acidity constants (Table 1) have been obtained from the spectrophotometric titration curves measured at 298 K as described in the "Experimental" section. During the titration the formation of two families of spectral curves has been observed, and each of them had its own set of isobestic points. Increase of the DBU concentration on the solution led to the sequential formation of mono-and doubly deprotonated forms of studied porphyrins with acidity constants K_{a2} and K_{a1}, respectively. The spectral evolution in the Soret band region is presented on Fig. 1, and the corresponding titration curves are shown on Fig. 2.

The overall acidity constant for complete deprotonation of macrocycle $pK_{a1,2}$ (Table 1) was calculated with Eq. 1:

$$pK_{a1,2} = n \times lg\, C_{DBU} - -lg\, Ind, \qquad (1)$$

where, Ind is the indicator of concentration ratio $[P^{2-}]/[H_2P]$, C_{DBU} is analytic value of the DBU in solution (mole L^{-1}), $n = 2$ is the total number of the protons attached. The calculations of the current concentrations of mono- and doubly deprotonated forms and free base species, taking into account the material balance equation $C_0 = C(H_2P) + C(HP^-) + C(P^{2-})$, show that all the porphyrins reached the doubly deprotonated form at the end of titration procedure. The measured $pK_{a1,2}$ values (Table 1) reveal the substantial difference depending the type of substitution. The acidity values must correlate with the electronic density on the pyrrole nitrogens. The way how the peripherical substituents influence it remain unclear. It was demonstrated that both resonance and inductive effects bring the contributions to the given basicity constant of macrocycle [17]. From general point of view the same should be valid for the acidity constant. The complication arises that in the above cited case the only substitution type contributes, whereas in the case under consideration both *meso*- and pyrrole ring *β*-substitutions are involved. Therefore, the overall substitution effect (for both *meso*- and *β*-positions) was calculated as a weighted sum of the resonance $\Sigma\sigma_R$ and inductive $\Sigma\sigma_I$ Hammett constants over all the substituents. The least-square fitting procedure was applied to evaluate the relative weights of these two terms assuming the linear dependence of the acidity constant on the value $a_1\Sigma\sigma_R + a_2\Sigma\sigma_I$, according to the linear free energy relationship. The resonance Hammett constants σ_R were calculated by subtraction of inductive Hammett constants σ_I from the Hammett *para*-constant σ_p according to definition, with both taken from literature [18].

The dependence shown on Fig. 3 clearly demonstrates that the acidity constant value correlates perfectly with the weighted sum $a_1\Sigma\sigma_R + a_2\Sigma\sigma_I$, with the weight coefficients a_1 and a_2 are 0.59 and 0.41, respectively. Neither resonance nor inductive effects alone can provide the satisfactory correlation with the measured acidity values. It is evident that both
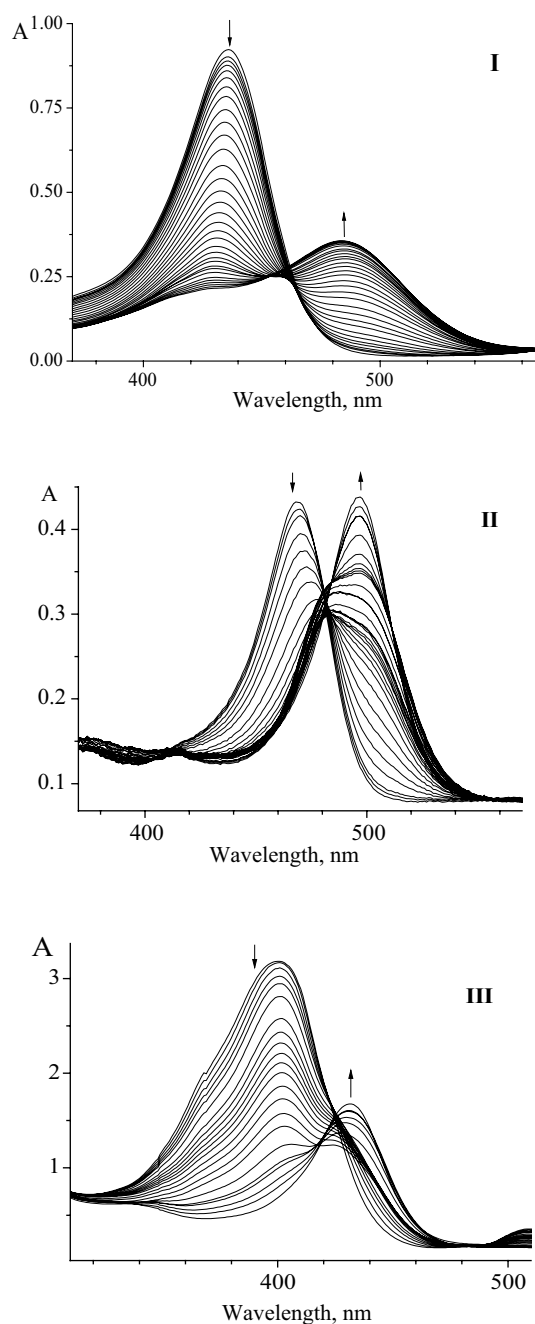

Fig. 1 Ground state absorption spectra changes in the Soret band region in the course of the titration of porphyrins **I**–**III** (from *top* to *bottom*) with the DBU in acetonitrile at 298 K: **I** $C_p = 1.2 \times 10^{-5}$ mole L^{-1}; $C_{DBU} = 0$–1.4×10^{-3} mole L^{-1}; **II** $C_p = 2.4 \times 10^{-6}$ mole L^{-1}; $C_{DBU} = 0$–5.0×10^{-5} mole L^{-1}; **III** $C_p = 1.9 \times 10^{-5}$ mole L^{-1}; $C_{DBU} = 0$–7.9×10^{-3} mole L^{-1}. Arrows indicate the direction of spectral changes upon DBU addition

resonance and inductive effects strongly contribute to the acidity constant $pK_{a1,2}$ with slightly larger part is due to the propagation of electronic communication via π-conjugated system. To achieve the more generalized correlation the plot shown on Fig. 3 consists of an additional data point for the
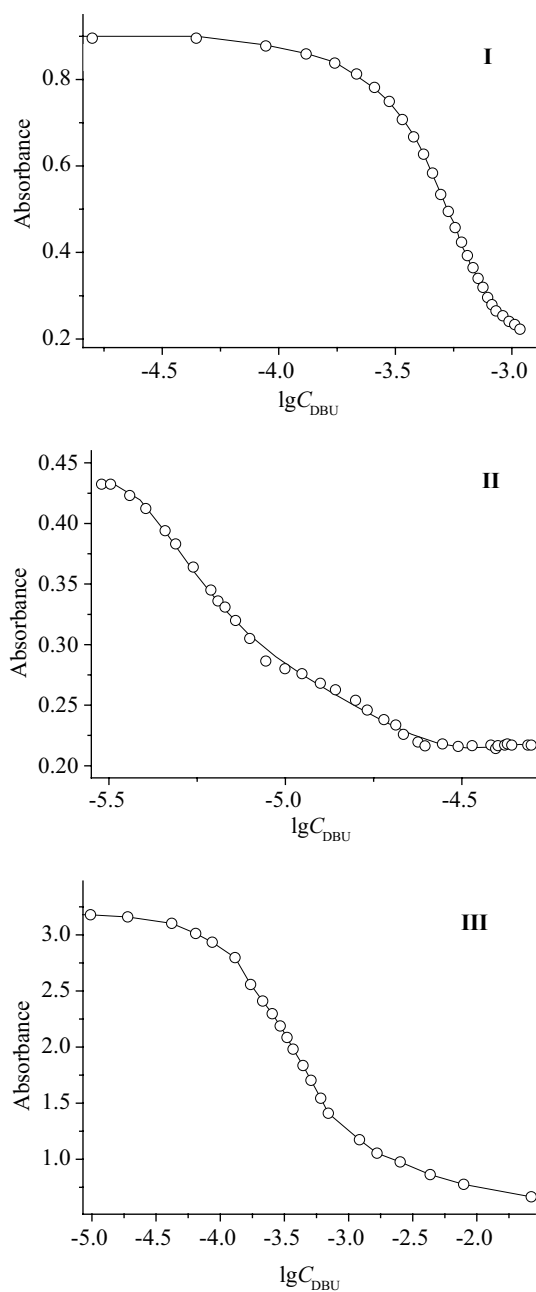
Fig. 3 The correlation plot of porphyrin $pK_{a1,2}$ and the weighted sum of the resonance $\sum\sigma_R$ and inductive $\sum\sigma_I$ Hammett constants of macrocycle substituents according to equation $0.59(8\sigma^\beta + 4\sigma^{meso})_R + 0.41(8\sigma^\beta + 4\sigma^{meso})_I$. The open circle (**H₂PIV**) relates to the 5,10,15,20-tetranitro-2,3,7,8,12,13,17,18-octaethylporphyrin whose $pK_{a1,2} = 10.44$

It is worthwhile to note that phenyl ring and bromine in porphyrin **II** contribute to the achieved balance in the complicated manner, since their resonance Hammett constants are negative (i.e. have resonance electron donating character), whereas inductive Hammett constants are positive (i.e. have inductive electron withdrawing properties). It is the derivative that demonstrates the highest complexation rate for both the free bases and doubly protonated molecules.

Acidity and complexation of Zn^{2+} ion

As was indicated above, the molecular structure of the porphyrin macrocycle is crucial for the rate of the metal ion chelating in the macrocycle core. Formation of nonplanar conformers is expected to bring for increase in the complexation rate and enhancement of both acidic and basic properties of molecule [13, 14, 20, 21]. The results of the measurements of the kinetic parameters of Zn^{2+} ion complexation with studied porphyrins meet this expectation (Table 2).

However, as we have stressed above, the driving force for the spectral changes as well as for the changes in the reactivity of tetrapyrrolic compounds originates from the electronic effects, both direct and indirect (i.e. electronic effects induced by structural changes). To verify this suggestion we have analyzed the second-order rate constant k_2 for the Zn^{2+} ion complexation by free base porphyrins as a function of the acidity ($pK_{a1,2}$). The obtained correlation plot is shown on Fig. 4 (the data point for the 5,10,15,20-tetranitro-2,3,7,8,12,13,17,18-octaethylporphyrin included). One can see that the excellent agreement exists between two sets of data. This means that the

Fig. 2 Titration curves for porphyrins **I**–**III** (for conditions see Fig. 1 caption). Titration wavelengths are: **I** 435 nm; **II** 469 nm; **III** 400 nm. DBU concentration is in mole L^{-1} units. Deprotonation of porphyrins is in going from left to right. Lines represent the calculated theoretical curves

5,10,15,20-tetranitro-2,3,7,8,12,13,17,18-octaethylporphyrin (denoted on the figure as **H₂PIV**) which has been taken from our recently published paper [19]. We need to stress once again that all the data in plot are measured for either nearly planar or having moderately distorted macrocycle derivatives. Strong nonplanar distortions of macrocycle cause the deviations from this relationship (see below).
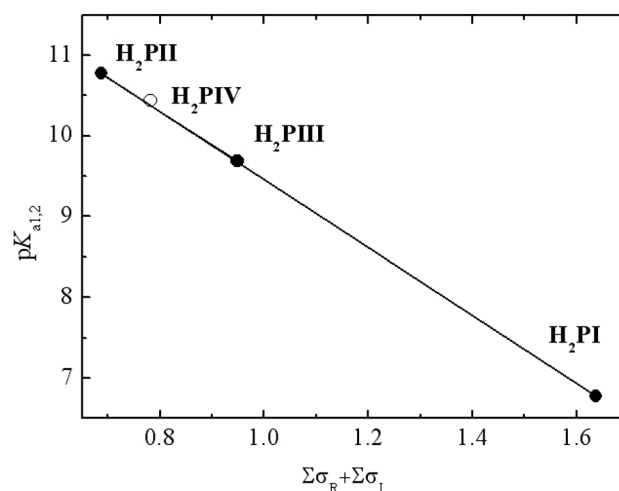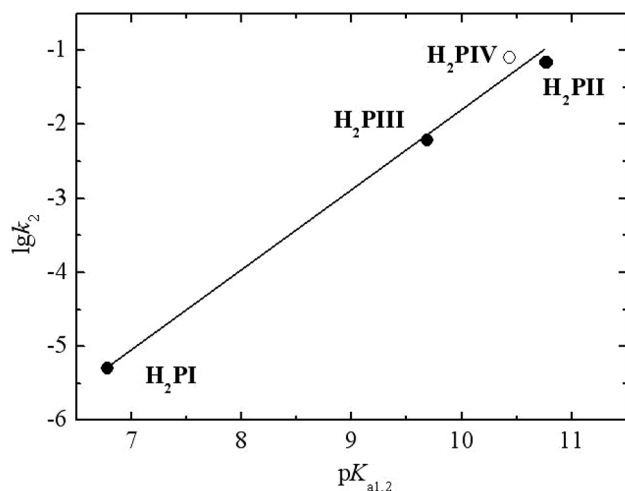
Table 2 Kinetic parameters of the Zn^{2+} ion complexation for all the studies porphyrins

Compound	$c_{Zn(QAc)2} \times 10^3$, mole L^{-1}	$c_{DBU} \times 10^3$, mole L^{-1}	$k_2 \times 10^3$, L mole^{-1} s^{-1}	E_a, kJ mole^{-1}	$\Delta S^{\neq}$, J mole^{-1} K^{-1}
H₂PI	4.5	–	0.005 ± 0.0005	123 ± 2	58 ± 1
H₂PII	4.5	–	69 ± 1	56 ± 1	-88 ± 2
H₂PIII	11.4	–	6.1 ± 0.1	52 ± 2	-175 ± 2
PI²⁻	4.5	1.5	28.0 ± 0.2	27 ± 1	-190 ± 2
PII²⁻	4.5	0.05	Completed immediately		
PIII²⁻	0.28	1	4006 ± 5	24 ± 1	-143 ± 2

Fig. 4 The dependence of second-order rate constant k_2 (in L mole^{-1} s^{-1}) for the Zn^{2+} ion complexation by the free base porphyrins on $pK_{a1,2}$ value. The open circle (**H₂PIV**) relates to the 5,10,15,20-tetranitro-2,3,7,8,12,13,17,18-octaethylporphyrin ($k_2 = 81 \times 10^{-3}$ L mole^{-1} s^{-1})

increase in the acidity value is able to explain completely increase in the Zn^{2+} ion complexation rate by these free base porphyrins for $pK_{a1,2}$ values ranging within four orders of magnitude.

Recently reported Zn^{2+} ion complexation rate $k_2 = 18$ L mole^{-1} s^{-1} and the value of $pK_{a1,2} = 11.65$ for the highly distorted 5,10,15,20-tetraphenyl-2,3,7,8,12,13,17,18-octamethylporphyrin follow the observed trends too [20]. However the data points deviate from the strict linear dependences revealed on Figs. 3 and 4. Most likely, it could be due to the high pyrrole tilting angles for this derivative, since the highly tilted pyrroles lead to decrease in the strength of the resonance electronic communication between the periphery and π-conjugated macrocycle system, which leads to alterations in the proportion (changing weigths) between the resonance and inductive contributions to the $pK_{a1,2}$ value. As a result, the $pK_{a1,2}$ value will be lower than it could be expected according to proportionality with the weighted sum $a_1\Sigma\sigma_R + a_2\Sigma\sigma_I$.

An increase in the complexation rate is also observed for the doubly deprotonated species. The activation energy value in case of deprotonated species decreases compared to that measured for the complexation of the free base porphyrins, which is followed with entropy decrease (Table 2). These features are likely to be due to absence of the energy losses required for deformation and rupture of the N–H bonds in the porphyrin core, as well as due to nonuniform charge distribution over the macrocycle, leading to polarization of the electronic cloud. As a result, the doubly deprotonated porphyrins may have higher solvation in the transition state which facilitates the metal ion chelation.

It needs to be stressed that in case of the free base porphyrins an increase in the rate in going form porphyrin **I** to porphyrin **III** is 1210 times, and for the doubly deprotonated species increase is almost ten times less (Table 2). This difference can be accounted, probably, with changes in the electronic structure between the free base and corresponding deprotonated species. Thus, its known that two singlet one electron configurations $^1(b_{1u}e_g)$ and $^1(a_ue_g)$ mix efficiently via configuration interaction [22]. The amount of mixing can be subtly tuned with relatively small structural alterations, like changes in the dihedral angles between the macrocycle plane and those of the aromatic substituents, or pyrrole tilting in the nonplanar macrocycle conformers due to concomitant electronic density redistribution over the molecule [22, 23]. The changes in the configuration interaction can be estimated based on the wavefunction superposition principle. This approach (see "Appendix" for detail) was first applied for the porphyrin metallocomplexes [24], and was extended recently by us for the free bases and the doubly protonated species [23].

Thus, the treatment of the spectral data for the porphyrin **III** with this approach results in the A^2 value (weight squared) for $^1(a_ue_g)$ configuration of 0.80 in the free base form, whereas it slightly increases up to 0.84 for the doubly deprotonated molecules. These estimations indicate that the changes in the electronic communication between the macrocycle and periphery take place indeed upon proton removal and may influence the metal ion complexation rate for the doubly deprotonated porphyrins. To make more

conclusive suggestion, additional studies need to be undertaken which need to involve an extended series of porphyrin derivatives.

Conclusion

Doubly deprotonated forms of three porphyrin derivatives have been obtained with DBU titration in acetonitrile solutions at room temperature. The reaction of both free bases and doubly deprotonated forms with zinc diacetate was investigated. The formation of Zn^{2+} metallocomplexes in both cases was found to occur. The second-order reaction rate constant of metallocomplexes formation was shown to increase by three to four orders of magnitude for deprotonated form of porphyrins compared to their free bases. The linear relationship between this reaction rate constant measured for the free bases and the overall acidity constant $pK_{a1,2}$ for porphyrin macrocycle deprotonation was demonstrated. The $pK_{a1,2}$ value was found to depend on both resonance and inductive electronic communication between macrocycle and its peripheral substituents. The adjustment of the electronic communication between macrocycle and periphery in going from the free bases to the doubly deprotonated species is reported based on the configuration interaction estimations from the Gouterman four-orbital model.

Considering the doubly deprotonated species as the promising candidate compounds to design the sensitive metal ion sensors, the obtained results allow suggesting the guidelines for the enhancement of their sensitivity.

Appendix

Estimation of one electron configuration mixing weights

Using the superposition principle one can write the wave function of two (doubly degenerated) excited states $S_{1,2}(Q)$ and $S_{3,4}(B)$ as:

$$\psi(S_{1,2}) = A\,^1\psi_A - B\,^1\psi_B (A^2 + B^2 = 1),$$

$$\psi(S_{3,4}) = B\,^1\psi_A + A\,^1\psi_B,$$

where A и B are the weights of the former and latter one electron configurations, respectively. The absorptivity of corresponding electronic transitions is given as:

$$I(S_{1,2}) = c|\langle\psi(S_1)|er|\psi(S_1)\rangle|^2 = c\{A^2\Phi_{AA} - 2AB\Phi_{AB} + B^2\Phi_{BB}\},$$

$$I(S_{3,4}) = c|\langle\psi(S_2)|er|\psi(S_2)\rangle|^2 = c\{A^2\Phi_{AA} + 2AB\Phi_{AB} + B^2\Phi_{BB}\},$$

where

$$\Phi_{AA} = \langle\,^1\psi_A|er|\,^1\psi_A\rangle,$$
$$\Phi_{AB} = \langle\,^1\psi_A|er|\,^1\psi_B\rangle,$$
$$\Phi_{AB} = \langle\,^1\psi_B|er|\,^1\psi_B\rangle.$$

Assuming the dipole moments of two one electron transitions are of the same order of magnitude,

$$Mae = \langle\,^1(b_{1u}e_g)|er|\,^1(b_{1u}e_g)\rangle \approx \langle\,^1(a_u e_g)|er|\,^1(a_u e_g)\rangle$$

and assigning $\psi_A = (b_{1u}e_g)$ and $\psi_B = (a_u e_g)$, the simple relationship for the intensities of these two electronic transitions can be written. It is given with the weights of two one electron configurations:

$$\frac{I(S_{1,2})}{I(S_{3,4})} = \frac{A^2 - 2AB + B^2}{A^2 + 2AB + B^2} = \frac{1 - 2AB}{1 + 2AB}.$$

After solving the system of algebraic equations (taking into account the normalization: $A^2 + B^2 = 1$) one can find the squared configuration weights A^2 and B^2.

References

1. Senge, M.O.: Excercises in molecular gymnastics - bending, stretching and twisting porphyrins. Chem. Commun. **3**, 243–256 (2000)
2. Berezin, B.D.: Coordination Compounds of Porphyrins and Phthalocyanines. Wiley, New York (1981)
3. Davis, D.J., Electrochemistry of porphyrins. In: Dolphin, D. (ed.) The Porphyrins, vol. 5, p. 127. Academic Press, New York (1978)
4. Phillips, J.N.: Physico-Chemical Properties of Porphyrins. In: Florkin, M., Stotz, E. (eds.) Comprehensive Biochemistry, pp. 34–73. Elsevier, Amsterdam (1963)
5. Andrianov, V.G., Malkova, O.V.: Acid-base properties of porphyrins in non-aqueous solution. Macroheterocycles. **2**, 130–138 (2009)
6. Kruk, M.M., Starukhin, A.S., Maes, W.: Influence of macrocycle protonation on the photophysical properties of porphyrins. Macroheterocycles. **4**, 69–79 (2011)
7. Ivanova, Y.B., Chizhova, N.V., Kruk, M.M.: Spectrophotometric study of 2,3,12,13-tetrabromo-5,10,15,20-tetraphenylporphyrin in the system 1,8-diazabicyclo[5.4.0]undec-7-ene- acetonitrile at 298 K. Deprotonation of the pyrrole rings and complex formation with Zn(OAc)$_2$. Russ. J. Gen. Chem. **83**, 558–563 (2013)
8. Ivanova, Y.B., Nam, D.T., Syrbu, A.S., Kruk, M.M.: Formation of phthalocyanines deprotonated forms and their interaction with Zn Ions in the system 1,8-diazabicyclo[5.4.0]undec-7-ene-acetonitrile at 298 K. Russ. J. Gen. Chem. **83**, 1155–1159 (2013)
9. Nam, D.T., Ivanova, Y.B., Pukhovskaya, S.G., Syrbu, A.S., Kruk, M.M.: Acid-base equilibria and coordination chemistry of the

5,10,15,20-tetraalkyl-porphyrins: implications for metalloporphyrin synthesis. RSC Adv. **5**, 26125–26131 (2015)

10. Ivanova, Y.B., Chourakhina, Y.I., Kumeev, R.S., Mamardashvili, M.Z., Semeikin, A.S.: Synthesis and basic properties of 5-aza-2,3,7,8,12,13,17,18-octamethylporphyrin. Russ. J. Gen. Chem. **78**, 1972–1976 (2008)

11. He, C.L., Ren, F.L., Zhang, X.B., Han, Z.X.: A fluorescent chemical sensor for Hg(II) based on a corrole derivative in a PVC matrix. Talanta. **70**, 364–370 (2006)

12. Pukhovskaya, S.G., Efimovich, V.A., Semeikin, A.S., Kolodina, E.A., Golubchikov, O.A.: Electronic and steric effects of substituents on the coordinating properties of porphyrins. Russ. J. Gen. Chem. **82**, 476–484 (2012)

13. Senge, M.O., Kalish, W.W.: Synthesis and structural characterization of nonplanar tetraphenylporphyrins and their metal complexes with graded degrees of β-ethyl substitution. Inorg. Chem. **36**, 6103–6116 (1997)

14. Shelnutt, J.A., Song, X.-Z., Ma, J.-G., Jia, S.-L., Jentzen, W., Medforth, C.J.: Nonplanar porphyrins and their significance in proteins. Chem. Soc. Rev. **27**, 31–41 (1998)

15. Parusel, A.B.J., Wondimagegn, T., Ghosh, A.: Do nonplanar porphyrins have red-shifted electronic spectra? A DFT/SCI study and reinvestigation of a recent proposal. J. Am. Chem. Soc. **122**, 6371–6374 (2000)

16. Haddard, R.E., Gazeau, S., Pecaut, J., Marchon, J.-C., Medforth, C.J., Shelnutt, J.A.: Origin of the red shifts in the optical absorption bands of nonplanar tetraalkylporphyrins. J. Am. Chem. Soc. **125**, 1253–1268 (2003)

17. Meot-Ner, M., Adler, A.D.: Substituent effects in noncoplanar π-systems. ms-Porphins. J. Am. Chem. Soc. **97**, 5107–5711 (1975)

18. Murov, S.L., Carmichael, I., Hug, G.L.: Handbook of photochemistry, 2nd edn., pp. 345–348. Marcel Dekker, New York (1993)

19. Ivanova, Yu.B., Chizhova, N.V., Mamardashvili, N.Z., Pukhovskaya, S.G.: Influence of substituents structure and their electronic effects on acid-base and complexing properties of 5,10,15,20-tetranitro-2,3,7,8,12,13,17,18-octaethylporphyrin. Russ. J. Gen. Chem. **84**, 939–945 (2014)

20. Ivanova, Y.B., Mamardashvili, N.Z., Nam, D.T., Glazunov, A.V., Semeykin, A.S., Pukhovskaya, S.G.: Synthesis and spectrophotometric study of deprotonation of octamethylporphyrin derivatives with 1,8-diazabicyclo[5.4.0]undec-7-ene in acetonitrile. Russ. J. Gen. Chem. **84**, 103–107 (2014)

21. Berezin, B.D., Ivanova, Y.B., Sheinin, V.B.: The acid properties of dodecasubstituted porphyrins with a chemically active NH bond. Russ. J. Phys. Chem. **81**, 1986–1991 (2007)

22. Gouterman, M.: Optical Spectra and Electronic Structure of Porphyrins and Related Rings. In: Dolphin, D. (ed.) The Porphyrins, vol. 3, pp. 1–165. Academic Press, New York (1978)

23. Liulkovich, L.S., Kruk, M.M.: Configuration interaction upon nonplanar distortions of the tetrapyrrolic macrocycle. Proceedings of Belarusian State Technological University (BSTU). **170**(**6**), 63–67 (2015)

24. Yamauchi, S., Matsukawa, Y., Ohba, Y., Iwaizumi, M.: State mixing in the excited triplet and singlet states of fluorine-substituted magnesium tetraphenylporphines studied by optical and time-resolved EPR spectroscopy. Inorg. Chem. **35**, 2910–2914 (1996)